



This open access document is posted as a preprint in the Beilstein Archives at <https://doi.org/10.3762/bxiv.2021.4.v1> and is considered to be an early communication for feedback before peer review. Before citing this document, please check if a final, peer-reviewed version has been published.

This document is not formatted, has not undergone copyediting or typesetting, and may contain errors, unsubstantiated scientific claims or preliminary data.

Preprint Title Borylated methyl cinnamates: Expedited synthesis, characterization, crystallographic analysis and biological activities in glycosidase inhibition and in cancer cells lines.

Authors William J. Legge, Yuna Shimadate, Mahdi Ghorbani, Jennette Sakoff, Todd A. Houston, Atsushi Kato, Paul Bernhardt and Michela I. Simone

Publication Date 22 Jan. 2021

Article Type Letter

Supporting Information File 1 Supp_information.docx; 3.0 MB

ORCID® IDs Jennette Sakoff - <https://orcid.org/0000-0002-7009-5792>; Todd A. Houston - <https://orcid.org/0000-0001-9369-8804>; Atsushi Kato - <https://orcid.org/0000-0001-8022-196X>; Michela I. Simone - <https://orcid.org/0000-0002-1339-8236>

Borylated methyl cinnamates: Expedited synthesis, characterization, crystallographic analysis and biological activities in glycosidase inhibition and in cancer cells lines.

William J. Legge,^{1,2} Yuna Shimadate,³ Mahdi Ghorbani,^{1,2} Jennette Sakoff,^{2,4} Todd A. Houston,⁵ Atsushi Kato,³ Paul V. Bernhardt,⁶ and Michela I. Simone^{1,2,*}

Address: ¹Discipline of Chemistry, University of Newcastle, Callaghan, NSW 2308, Australia, ²Priority Research Centre for Drug Development, University of Newcastle, Callaghan, NSW 2308, Australia, ³Department of Hospital Pharmacy, University of Toyama, 2630 Sugitani, Toyama 930-0194, Japan, ⁴Calvary Mater Newcastle Hospital, Edith Street, Waratah, NSW 2298, Australia, ⁵Institute for Glycomics and School of Natural Sciences, Griffith University, Gold Coast Campus, Southport, QLD 4222, Australia and ⁶School of Chemistry and Molecular Biosciences, University of Queensland, Brisbane 4072, Australia.

Email: Michela Simone - michela.simone@newcastle.edu.au, michela_simone@yahoo.co.uk.

Abstract

Three cinnamate derivatives bearing a boronate pinacol ester group *para*, *meta* and *ortho* to the α,β -unsaturated ester group have been synthesized *via* a solventless, expedited Wittig protocol in the best stereoisomeric ratios yet reported, purified by recrystallization, characterized and analyzed by X-ray crystallography. These are valuable building blocks to biologically active derivatives and are themselves biologically active drug leads, displaying excellent selectivities as glycosidase modulators and for future testing as boron neutron capture therapy (BNCT)

agents. In a panel of 15 glycosidases, IC₅₀ values of 351 μM and 374 μM were shown for **para 2** against almond β-glucosidase and bovine liver β-galactosidase, respectively. For **meta 2** the selectivity profile is improved with only inhibition of bovine liver β-galactosidase with an IC₅₀ of 780 μM. These borylated derivatives also possess the capability to be used as BNCT agents. This occurs via irradiation with slow neutrons, thus granting them a switch-on/switch-off toxicity. This is an important new capability imbued into anticancer drugs, too many of which are too toxic in their therapeutic window. BNCT drugs bearing the organic boron pharmacophore have the potential to fine-tune the timing of toxicity delivery.

Keywords

Cinnamate, pinacol boronate ester, Wittig reaction, X-ray crystallography, glycosidase, boron neutron capture therapy, accumulation selectivity in cancer vs healthy cells

Synopsis

Reported is the efficient syntheses to novel drugs for medicinal chemistry applications in the areas of broad-spectrum anticancer agents and glycosidase inhibitors.

Introduction

The Wittig Reaction, with its variations (e.g. the Horner-Wadsworth-Emmons (HWE) reaction), provides a particularly reliable synthetic tool for the stereocontrolled formation of ethylenic bonds. It allows preparation of an alkene by reaction of an aldehyde or ketone with the ylide generated from a phosphonium salt.¹ The geometry of the resulting alkene depends on the reactivity of the ylide. If the ylide is stabilized by an electron-withdrawing group then

predominantly (*E*)-alkenes are formed. Non-stabilized ylides lead to (*Z*)-alkenes. The flexibility of the reaction allows to obtain simple as well as substituted molecular scaffolds.^{2,3} In the HWE reaction, the carbonyl compound of aldehydes or ketones reacts with stabilized phosphorus ylides (phosphonate carbanions) leading to olefins with excellent *E*-selectivity. The nucleophilic carbon needs to bear an anion stabilizing group (e.g. CO₂Me, COMe, COH, phenyl).

In our research laboratory we are interested in methodology development to the introduction of organic boron pharmacophores (in particular boronate esters and boronic acids) on biologically active molecular scaffolds.⁴⁻⁶ Cinnamic acid - with several of its analogues in the clinic, ozagrel, cinromide and piplartine (Figure 1) - represents one such structure possessing wide-ranging biological activity,⁷⁻¹² inclusive of glycosidase inhibitory capability.¹³⁻¹⁵

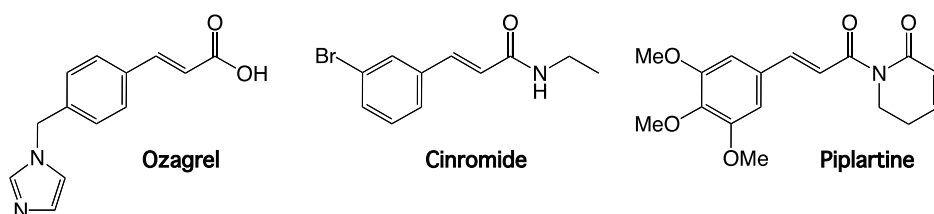


Figure 1. Cinnamic acid analogues in the clinic: ozagrel, cinromide and piplartine.

Results and Discussion

The Wittig and HWE reactions are a mainstay reaction in organic synthesis and provides a useful synthetic strategy to access cinnamic acid analogues. There are limited green solventless Wittig reaction protocols to the production of substituted cinnamate scaffolds. These involve either 1) a milling protocol by ball-milling,¹⁶ or grinding,¹⁷⁻²⁰ or 2) simply stirring.²¹⁻²³ Although non-green reaction solvents were eliminated from reaction protocols, however they tend to be used during purifications involving mostly column chromatography on silica, where copious amounts of solvents tend to be used (Table 1, Supporting Information) compared to the re/crystallization protocols used by us.

Ball-milling protocols include one-pot preparation of stabilized ylides followed by

solventless Wittig reaction in 8-20 hours under an atmosphere of helium and product (with *E:Z* ratio 3.5:1 to 1.6:1) isolation via column chromatography.¹⁶ The grinding of reactants with stabilized ylids provides mainly (*E*)-products, where isolation is achieved via recrystallization or column chromatography.¹⁷⁻²⁰ (*Z*)-Intermediates are produced only when coumarin target molecules were produced from reagents impregnated with sodium methoxide and magnesium oxide.¹⁸

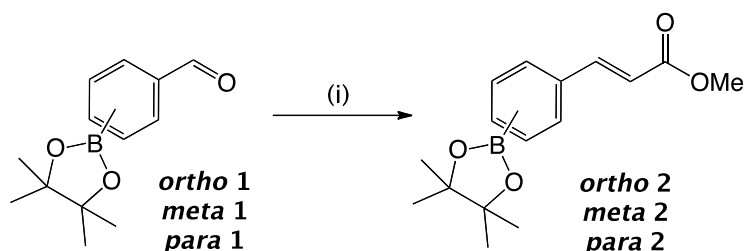
Under simple stirring conditions, the reaction can be carried out at room temperature with liquid aldehydes (e.g. benzaldehyde)²³ or, if heated, in a melt when using solid aldehydes,²³ e.g. 9-anthraldehyde.^{21,24,25} Microwave irradiation can also be applied to accelerate reaction rates provided phosphorane^{23,26} or phosphazene²⁷ stability. In dry conditions, the Wittig reaction has also been shown to occur in the presence of alumina or potassium fluoride supported on alumina, which after stirring for 48 hours afforded the alkene products in a *E:Z* ratio 92:8 to 1:1.²²

In many cases the easiest way of separating the excess phosphorane and triphenylphosphine byproduct is still column chromatography using non-green solvents.²⁵

In our laboratory, we have a strong interest in organic boron⁶ and the development of synthetic protocols to new drug leads containing organic boron pharmacophores.^{4,5,28} In the synthesis of methyl cinnamate analogues (Scheme 1), a solventless Wittig reaction, modified from two original procedures^{17,21} was employed with optimized reaction times and temperatures to ensure the rapid and efficient synthesis of boronate esters ***ortho 2***, ***meta 2*** and ***para 2*** in the set of highest stereoisomeric ratios to date in literature, followed by isolation by recrystallization or flash chromatography.

The rapid green olefination of ***ortho 2***, ***meta 2*** and ***para 2*** was effected with stabilized Wittig reagent (methoxycarbonylmethylene)triphenylphosphorane (Scheme 1) under normal atmosphere in an open round-bottom flask in a melt at 150°C for 2.5 hours to give the

corresponding methyl cinnamate products in 85, 89 and 91% yields respectively after purification via recrystallization in the best set of *E:Z* ratios in the literature, with 92.5:7.5, 99:1 and 92:8 respectively. Flash chromatography was also scoped out as a purification method that resulted in no loss of borylated products on silica. Flash chromatography can make purifications challenging in many cases due to over-adsorption of boron-containing compounds on silica, resulting in a reduction in yields.²⁹



Scheme 1. Reagents and Conditions: (i) (methoxycarbonylmethylene)triphenylphosphorane, 150°C, 2.5 hrs.

One literature protocol to the synthesis of ***ortho 2*** is known to proceed via stirring in toluene at 90°C for 18 hours, followed by purification by flash chromatography to give the product in an 87% yield, and in a *E:Z* ratio 85:15 as a light yellow solid. A pure sample of the *E*-isomer was obtained by recrystallization from hexanes and characterised by HRMS, IR, ¹H- and ¹³C-NMR.³⁰ Our ***ortho 2*** product's IR and NMR data match the literature data, apart from the location of the two pinacol C_q, at 77.5 ppm, whereas others³⁰ report them at 84.1 ppm.

One literature protocol to the synthesis of ***para 2*** (used as intermediate towards a-aminoquinazolin-4(3*H*)-ones as plasmepsin inhibitors) involves coupling of methyl (*E*)-3-(4-bromophenyl)acrylate (1.0 eq) with bis(pinacolato)diboron (1.2 eq) using Pd(dppf)Cl₂CH₂Cl₂ (0.1 eq) and KOAc (3.0 eq) in DMSO at 80°C under an argon atmosphere, which - after extraction, drying and purification by flash-chromatography - gave the product in 52% yield as a white

amorphous solid and was characterised by ^1H - and ^{13}C -NMR.³¹ Our product's NMR data match the literature data.

In related work, Molander and Oliveira carried out the Wittig reaction of aromatic organotrifluoroborates with methyl(triphenylphosphoranylidene) acetate in water at 90°C , with a 12 hour reaction time, to give the corresponding trifluoroborate methyl cinnamates in variable diastereoselectivities ($E:Z$ 70:30 (*para*), 100:0 (*meta*), 80:20 (*ortho*)) and isolated after trituration in DCM and acetone as mainly mixtures of *E* and *Z* products.³²

X-Ray Crystallography Data

As each of the three borylated cinnamates produced crystalline products, they were studied by X-ray crystallography. For ***ortho* 2** the alkene moiety is in a *trans* configuration and the dioxaborolane 5-membered ring is in a puckered conformation with atoms C2A, B1A, O3A and O4A sitting on the same plane in trigonal planar geometry with angle O3A-B1A-C2A measuring the ideal $120.07(13)^\circ$, whereas angles O4A-B1A-O3A and O4A-B1A-C2A departing by $\sim 6^\circ$ from the ideal trigonal planar geometry angle and measuring respectively $113.34(12)^\circ$ and $126.59(13)^\circ$; the dihedral angle B1A-C2A-C1A-C7A measures 20° thus displacing the pinacol ester group from the plane on which the aromatic ring and the α,β -unsaturated ester lie. Furthermore, ***ortho* 2** crystallised with two molecules in the asymmetric unit (labelled "A" and "B") which are essentially indistinguishable.

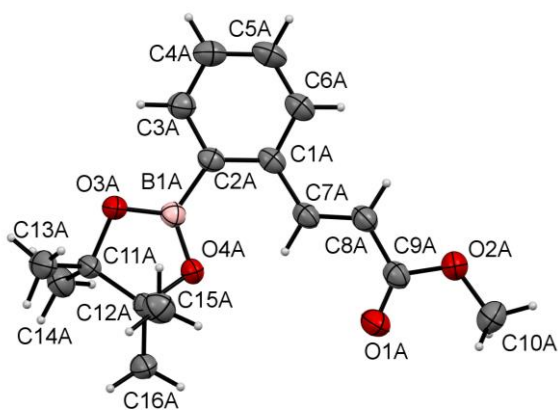


Figure 2. ORTEP Diagram of (*E*)-methyl 3-(2-(4,4,5,5-tetramethyl-1,3,2-dioxaborolan-2-yl)phenyl)acrylate *ortho 2*.

The arrangement of the four molecules in the unit cell (Supporting Information Figure S1) involves the two B molecules sitting on parallel planes, head-to-tail to one another, so that the aromatic and pinacol ester moieties of one molecule are facing one another. The two A molecules are also sitting on parallel planes in such a way that the aromatic moiety and the chain containing the α,β -unsaturated esters are facing head-to-tail to one another.

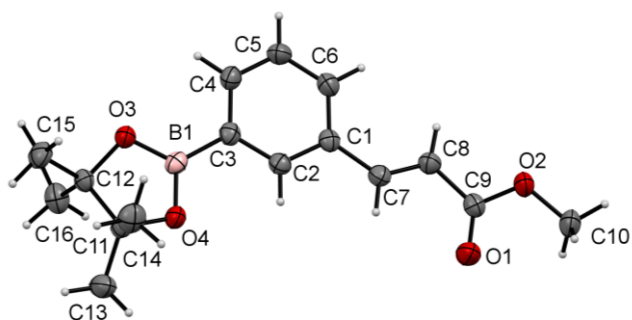


Figure 3. ORTEP Diagram of (*E*)-methyl 3-(3-(4,4,5,5-tetramethyl-1,3,2-dioxaborolan-2-yl)phenyl)acrylate *meta 2*.

In compound *meta 2* (Figure 3) the dioxaborolane ring is again in a puckered conformation. The alkene also retains its *trans* conformation. Each O-atom is involved in non-classical intermolecular H-bonding interactions with the strongest being to the carbonyl O1A which accepts C-H...O bonds of ~ 2.55 Å from C6A and C8A in addition to the methoxy group which donates a C-H...O bond (2.51 Å) to the pinacol O-atom O4 (Supporting Information Figure S2).

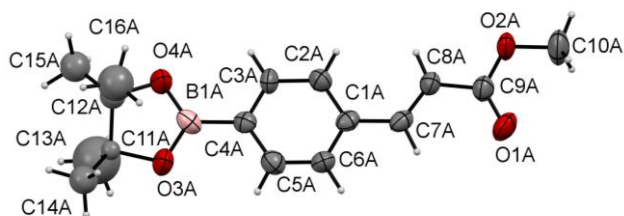


Figure 4. ORTEP Diagram of molecule A of the asymmetric unit of (*E*)-methyl 3-(4-(4,4,5,5-tetramethyl-1,3,2-dioxaborolan-2-yl)phenyl)acrylate ***para 2***. One of the two disordered conformations is shown.

There are two molecules in the asymmetric unit of the ***para 2*** structure and one of these is shown in Figure 4. The boronate ester groups were disordered between two different puckered conformations (Supporting Information Figure S3). Of the three geometrical isomers, ***para 2*** was the only one that suffered disorder. Similarly to ***meta 2***, the atoms forming the alkyl framework of both molecules in the asymmetric unit (C10 to B1) are sitting on the same plane (Figure 3). The alkene is in *trans* conformation in this case as well.

Glycosidase Assay

In our laboratory, we have an interest in the inhibition of glycosidases to the management of many disease types, including metabolism,³³ viral³⁴ and lysosomal storage disorders.³⁵ Cinnamates have been found to possess glycosidase inhibition properties¹³ as “neutral” (i.e. lacking a basic nitrogen found in iminosugars/azasugars) glycosidase inhibitors.¹⁵ Here the boron pinacol ester was explored as a pharmacophoric group in the *para*-, *meta*- and *ortho*-positions to the unsaturated ester on the aromatic ring. Organic boron continues to emerge as a pharmacophore capable of not only intermolecularly interacting with active sites, but also intramolecularly through the establishment of dative bonds from nucleophilic atoms of the enzyme to the electrophilic boron atom. Introduction of a boronic acid can shift the glycosidase inhibitory profile of an iminosugar.³⁶ Free boronic acids can also improve inhibition by forming

hydrogen bonds to an enzyme.³⁷ The kaleidoscopic chemistry associated with the organic boron atom grants huge potential in terms of the chemical and physical tuning of the drug molecule properties, but at the same time represents a huge challenge to the organic/medicinal chemist developing high Fsp³ index³⁸ boron-bearing drug leads.^{4,5,39,40}

In Table 1, the three boron-bearing leads **para 2**, **meta 2** and **ortho 2**, and the reference compound methyl cinnamate were screened against a panel of 15 glycosidases to assess both potency and selectivity of inhibition. It is shown that methyl cinnamate does not significantly inhibit any of the glycosidases assayed, with % inhibition at 1000 μ M ranging from 0% to 34%. **Ortho 2** has a similar inhibition profile to methyl cinnamate with % inhibition at 1000 μ M ranging from 0% to 42%. However, **meta 2** and **para 2** provide weak but highly or exclusively selective inhibition. The IC₅₀s are 351 μ M and 374 μ M for **para 2** against β -glucosidase (almond) and β -galactosidase (bovine liver) in a panel of 15 glycosidases. The positioning of the boron is clearly important for inhibition of the almond β -glucosidase but has no impact on the inhibition of bovine liver β -glucosidase as all four compounds only partially inhibit the enzyme to the same degree (ca. 30% at 1000 μ M). For **meta 2** the selectivity profile is improved with only inhibition of bovine liver β -galactosidase with an IC₅₀ of 780 μ M. The positioning of the boronate ester group in *para* and *meta* positions provides favourable interactions with selected β -glycosidases.

Cancer Assay

In our laboratory we are interested in the use of BNCT as a potentially broad-spectrum approach to cancer management. Providing the drugs can selectively accumulate in cancer cells vs healthy cells,⁴¹ it should be possible to manage the disease via BNCT, a non-invasive and least destructive radiation therapy currently available.⁴²⁻⁴⁴ In order to use a drug in BNCT, it is ideal if, when not irradiated, the drug is non-toxic. In this preliminary study of synthesis, purification and toxicity of organic boron containing drug leads for BNCT applications, none of

the three borylated derivatives were found to be toxic in cancer cells lines and a normal cell line (MCF10A) (Table 2). The organic boron pharmacophore provides promising results in this area because the currently in use BNCT agent sodium borocaptate, BSH, containing an inorganic boron pharmacophore, raises several toxicity concerns,⁴⁵⁻⁴⁶ whereas boronophenylalanine, BPA, which contains the organic boronic acid pharmacophore has long been known to show no discernible toxicity.⁴⁷ Organic boron is also an essential element for plants and is probably essential for human and animal health.⁴⁸ When comparing toxicological data for organic boron containing molecules with their non-borylated congeners, it is also found that in general the presence of organic boron lowers toxicity profiles. For example, benzene has a lethal dose (LD₅₀) = 125 mg/kg (human, oral)⁴⁹ and a lethal concentration (LC_{LO}) = 20,000 ppm (human, 5 min), it is carcinogenic, and also a possible mutagenic. The NIOSH Permissible Exposure Limit for benzene = 1 ppm, the Recommended Exposure Limit = 0.1 ppm, and the Immediately Dangerous to Life and Health concentration at 500 ppm].⁵⁰ Phenylboronic acid on the other hand has an LD₅₀ 740 mg/kg (rat, oral),⁵¹ with no entry for RTECS, ACGIH, IARC, or NTP. Our group has also recently achieved a more selective delivery of anticancer agents to cancer versus healthy cells.⁴¹

Table 2 shows the percentage (%) cell growth inhibition in response to 25µM of drug. The higher the value the greater the growth inhibition. A value of <0 indicates zero growth inhibition and most likely growth stimulation. None of the drug leads significantly inhibited cell growth of any of the cancer cell lines and of the normal cell line at the screened concentration value. **Ortho 2** showed zero growth inhibition towards U87, BE2-C and SMA560 cancer cell lines. Dose response experiments (GI₅₀ as concentration (µM) that inhibits cell growth by 50%) were not completed for these compounds.

Experimental

Glycosidase Assay Experimental

The enzymes α -glucosidase (from yeast), β -glucosidases (from almond and bovine liver), α -galactosidase (from coffee beans), β -galactosidase (from bovine liver), α -mannosidase (from Jack bean), β -mannosidase (from snail), α -L-rhamnosidase (from *Penicillium decumbens*), α -L-fucosidase (from bovine kidney), trehalase (from porcine kidney), β -glucuronidases (from *E. coli* and bovine liver), amyloglucosidase (from *A. niger*), *p*-nitrophenyl glycosides, and various disaccharides were purchased from Sigma-Aldrich Co. Brush border membranes were prepared from the rat small intestine according to the method of Kessler et al, and were assayed at pH 6.8 for rat intestinal maltase using maltose. For rat intestinal maltase, porcine kidney trehalase, and *A. niger* amyloglucosidase activities, the reaction mixture contained 25 mM maltose and the appropriate amount of enzyme, and the incubations were performed for 10-30 min at 37 °C. The reaction was stopped by heating at 100°C for 3 min. After centrifugation (600 g; 10 min), the resulting reaction mixture were added to the Glucose CII-test Wako (Wako Pure Chemical Ind., Osaka, Japan). The absorbance at 505 nm was measured to determine the amount of the released D-glucose. Other glycosidase activities were determined using an appropriate *p*-nitrophenyl glycoside as substrate at the optimum pH of each enzyme. The reaction mixture contained 2 mM of the substrate and the appropriate amount of enzyme. The reaction was stopped by addition of 400 mM Na₂CO₃. The released *p*-nitrophenol was measured spectrometrically at 400 nm.

Cancer Assay Experimental

All test agents were prepared as stock solutions (20 mM) in dimethyl sulfoxide (DMSO) and stored at -20 °C. Cell lines used in the study included HT29, (colorectal carcinoma); U87, SJ-G2, (glioblastoma); MCF-7, (breast carcinoma); A2780 (ovarian carcinoma); H460 (lung

carcinoma); A431 (skin carcinoma); Du145 (prostate carcinoma); BE2-C (neuroblastoma); MiaPaCa-2 (pancreatic carcinoma); and SMA560 (spontaneous murine astrocytoma); together with the one non-tumour derived normal breast cell line (MCF10A). All cell lines were incubated in a humidified atmosphere 5 % CO₂ at 37 °C. The cancer cell lines were maintained in Dulbecco's modified Eagle's medium (DMEM; Sigma, Australia) supplemented with foetal bovine serum (10 %), sodium pyruvate (10 mM), penicillin (100 IU mL⁻¹), streptomycin (100 µg mL⁻¹), and L-glutamine (2 mM). The non-cancer MCF10A cell line was maintained in DMEM:F12 (1:1) cell culture media, 5 % heat inactivated horse serum, supplemented with penicillin (50 IU mL⁻¹), streptomycin (50 µg mL⁻¹), HEPES (20 mM), L-glutamine (2 mM), epidermal growth factor (20 ng mL⁻¹), hydrocortisone (500 ng mL⁻¹), cholera toxin (100 ng mL⁻¹), and insulin (10 mg mL⁻¹).

Growth inhibition was determined by plating cells in duplicate in medium (100 µL) at a density of 2500-4000 cells per well in 96-well plates. On day 0 (24 h after plating), when the cells are in logarithmic growth, medium (100 µL) with or without the test agent was added to each well. After 72 h drug exposure, growth inhibitory effects were evaluated using the MTT (3-(4,5-dimethylthiazol-2-yl)-2,5-diphenyltetrazolium bromide) assay and absorbance read at 540 nm. The percentage growth inhibition was calculated at a fixed concentration of 25µM, based on the difference between the optical density values on day 0 and those at the end of drug exposure. Each data point is the mean ± the standard error of the mean (SEM) calculated from three replicates which were performed on separate occasions and separate cell line passages.

Chemistry Experimental

Reaction solvents were purchased from the Aldrich Chemical Company in sure-seal™ reagent bottles. All other solvents (analytical or HPLC grade) were used as supplied without further purification.

Reactions were performed in open round bottom flasks.

Reagents were used as provided, without further purification, provided an NMR analysis confirmed an acceptable degree of purity and correct identity of reagent.

Purification via silica gel column chromatography were performed on Davisil 40-63-micron silica gel.

Thin layer chromatography (t.l.c.) was performed on aluminium sheets coated with 60 F254 silica by Merck and visualised using UVG-11 Compact UV lamp (254 nm) or stained with the cerium molybdate stain (12.0 g ammonium molybdate, 0.5 g ceric ammonium molybdate in 15mL concentrated sulfuric acid and 235 mL distilled water).

Nuclear Magnetic Resonance (NMR) spectra were recorded on Bruker Ascend™ 400 in deuterated chloroform (CDCl₃). Chemical shifts (δ) are quoted in ppm and coupling constants (J) in Hz. Residual signals from the CDCl₃ (7.26 ppm for ¹H-NMR and 77.16 ppm for ¹³C-NMR) was used as an internal reference.⁵²

Infrared spectroscopy (IR) spectra were obtained on a PerkinElmer Spectrum Two Spectrometer and on a PerkinElmer Spectrum 2 with UATR. Only characteristic peaks are quoted and in units of cm⁻¹.

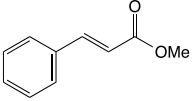
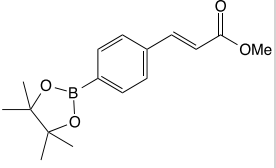
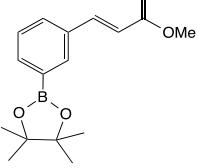
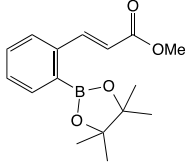
Infrared (IR) analyses were obtained on a PerkinElmer Spectrum Two Spectrometer and on a PerkinElmer Spectrum 2 with UATR. Only characteristic peaks are quoted and in units of cm⁻¹.

High Resolution Mass spectrometry (HRMS) spectra were obtained from samples suspended in acetonitrile (1 mL with 0.1% formic acid at a concentration of ~1 mg/mL, before being further diluted to ~10 ng/ μ L in 50% acetonitrile/water containing 0.1% formic acid). Samples were infused directly into the HESI source of a Thermo Scientific Q Exactive™ Plus Hybrid Quadrupole-Orbitrap™ Mass Spectrometer using an on-board syringe pump at 5 μ L/min. Data was acquired on the QE+ in both positive and negative ion mode at a target resolution of 70,000 at 200 m/z. The predominant ions were manually selected for MS/MS fragmentation (collision energies were altered for each compound to obtain sufficient fragmentation). Data analysis of each sample was performed manually using Thermo Qualbrowser whilst the Isotopic Patterns of predicted chemical formula were modelled using Bruker Compass Isotope Pattern.

Crystallographic data were obtained on an Oxford Diffraction Gemini CCD diffractometer employing either graphite-monochromated Mo-K α radiation (0.71073 Å) or Cu-K α (1.54184 Å). The sample was cooled to 190 K with an Oxford Cryosystems Desktop Cooler. Data reduction and empirical absorption corrections (multi-scan) were performed with Oxford Diffraction CrysAlisPro software. Structures were solved by direct methods with SHELXS and refined by full-matrix least-squares analysis with SHELXL.⁵³ All non-H atoms were refined with anisotropic thermal parameters except those involved in disorder which were refined isotropically with complementary occupancies. Molecular structure diagrams were produced with Mercury⁵⁴ and PLATON.⁵⁵ The data in CIF format has been deposited at the Cambridge Crystallographic Data Centre (CCDC 2015833-2015835). The crystals of **para 2** were non-merohedrally twinned and the structure was refined with the HKLF 5 facility within SHELX.

Melting points were taken on a DYNALON SMP100 Digital Melting Point Device and are uncorrected.

Table 1: Percentage inhibition data and IC₅₀ values (in red) for the most active drugs against a panel of 15 glycosidases.

enzyme	IC ₅₀ (μM)			
	Reference	<i>para</i> 2	<i>meta</i> 2	<i>ortho</i> 2
				
α-Glucosidase				
rice	^a NI ^b (2.7 %)	NI (5.3 %)	NI (6.8 %)	NI (21.2 %)
rat intestinal maltase	NI (6.0 %)	NI (0 %)	NI (9.0 %)	NI (0 %)
yeast	NI (3.0 %)	NI (0 %)	NI (42.0 %)	NI (0 %)
β-Glucosidase				
Almond	NI (6.7 %)	351	NI (16.5 %)	NI (9.8 %)
bovine liver	NI (33.6 %)	NI (31.0 %)	NI (32.0 %)	NI (29.4 %)
α-Galactosidase				
coffee beans	NI (10.0 %)	NI (5.4 %)	NI (7.1 %)	NI (0.7 %)
β-Galactosidase				
bovine liver	NI (32.1 %)	374	780	NI (42.5 %)
α-Mannosidase				
Jack bean	NI (5.5 %)	NI (1.4 %)	NI (3.1 %)	NI (3.1 %)
β-Mannosidase				
Snail	NI (0.3 %)	NI (0 %)	NI (0 %)	NI (0 %)
α-L-Fucosidase				
bovine kidney	NI (17.4 %)	NI (0 %)	NI (5.51 %)	NI (7.1 %)
α-L-Rhamnosidase				
<i>Penicillium decumbens</i>	NI (7.9 %)	NI (2.3 %)	NI (2.3 %)	NI (0 %)
Amyloglucosidase				
<i>A. niger</i>	NI (1.6 %)	NI (2.1 %)	NI (2.6 %)	NI (4.4 %)
Trehalase				
porcine kidney	NI (0.4 %)	NI (2.2 %)	NI (2.2 %)	NI (2.7 %)
β-Glucuronidase				
<i>E. coli</i>	NI (3.1 %)	NI (7.9 %)	NI (27.8 %)	NI (22.5 %)
bovine liver	NI (0 %)	NI (7.6 %)	NI (0.7 %)	NI (7.4 %)
	^a NI : No inhibition (less than 50% inhibition at 1000 μM).			
	^b () : inhibition % at 1000 μM			

Assays were also carried out against *N*-acetyl-β-D-glucosidase (bovine liver) at 1mg/mL in 10% DMSO showing values of 17.8%, 8.0%*, 12.8%* and 22.0%* respectively. *As suspension.

Table 2: Percentage (%) cell growth inhibition in response to 25µM of drug after 72 hour exposure using the MTT cell growth assay.

Cell Line	IC ₅₀ (mM)			
	Reference	<i>para</i> 2	<i>meta</i> 2	<i>ortho</i> 2
HT29, Colon carcinoma	12 ± 4	25 ± 6	27 ± 5	14 ± 5
U87, Glioblastoma	6 ± 4	6 ± 8	47 ± 5	0 ± 2
MCF-7, Breast carcinoma	31 ± 10	17 ± 10	20 ± 8	14 ± 7
A2780, Ovarian carcinoma	22 ± 5	27 ± 6	51 ± 4	18 ± 4
H460, Lung carcinoma	14 ± 8	17 ± 7	17 ± 5	8 ± 6
A431, Skin carcinoma	10 ± 8	17 ± 5	28 ± 2	5 ± 6
Du145, Prostate carcinoma	27 ± 6	9 ± 8	22 ± 10	10 ± 9
BE2-C, Neuroblastoma	1 ± 9	13 ± 3	41 ± 1	<0
SJ-G2, Glioblastoma	11 ± 2	23 ± 0	18 ± 4	15 ± 3
MiaPACa-2, Pancreatic carcinoma	11 ± 4	10 ± 3	22 ± 8	14 ± 5
SMA560, Glioblastoma (spontaneous murine astrocytoma)	6 ± 1	12 ± 5	8 ± 2	<0
MCF10A, Breast (normal)	8 ± 3	12 ± 5	22 ± 2	9 ± 2

The experiment was conducted in duplicate and replicated on three separate occasions.

(E)-Methyl 3-(2-(4,4,5,5-tetramethyl-1,3,2-dioxaborolan-2-yl)phenyl)acrylate *ortho* 2

2-(4,4,5,5-Tetramethyl-1,3,2-dioxaborolan-2-yl)benzaldehyde ***ortho* 1** (2.000 g, 8.618 mmol) was carefully added to

(methoxycarbonylmethylene)triphenylphosphorane (3.170 g, 9.479 mmol) stirring in a round bottom flask at r.t. The temperature was raised to 150°C and the powdery mixture liquefied and stirred as a pale yellow solution for 2.5 hours. The solution was allowed to cool down and turned into a tough pale yellow solid which was dissolved in DCM, transferred into a 500 mL round-bottom flask and evaporated in vacuo. TLC analysis (ethyl acetate/cyclohexane 1:4) revealed the presence of one product (Rf 0.70) and the byproduct triphenylphosphine oxide (Rf 0.10). Trituration with hexane and filtration allowed to remove a first crop of the byproduct triphenylphosphine oxide. The filtrate was left to stand overnight and a second crop of triphenylphosphine oxide crystallised. The hexane layer was decanted off and evaporated in vacuo and the product (*E*)-methyl 3-(4-(4,4,5,5-tetramethyl-1,3,2-dioxaborolan-2-yl)phenyl)acrylate ***ortho* 2** was recrystallized from diethylether or dissolved in diethylether and left to crystallise over a 24-hour period into big chunky crystals (2.111 g, 85%). NMR analysis revealed a *E:Z* ratio across the double bond of 92.5:7.5. M.p. 68-72°C. ¹H-NMR (400MHz, CDCl₃) δ 1.38 (s, 12H, 4 x CH₃), 3.81 (s, 3H, OCH₃), 6.38 (d, 1H, ³J_{H_α,H_β} 16.0 Hz, H_α-C=CH_β), 7.36 (td, 1H, ³J 7.4 Hz, ⁴J 0.8 Hz, ArH), 7.45 (td, 1H, ³J 7.4 Hz, ⁴J 1.2 Hz, ArH), 7.67 (d, 1H, ³J 7.6 Hz, ArH), 7.83 (dd, 1H, ³J 7.4 Hz, ⁴J 1.0 Hz, ArH), 8.57 (d, 1H, ³J_{H_β,H_α} 16.0 Hz, H_β-C=CH_α). ¹³C-NMR (100MHz, CDCl₃) δ 25.0 (4 x CH₃), 51.7 (OCH₃), 77.5 (2 x C_q-(CH₃)₂), 118.7 (H_βC=CH_α), 125.8, 129.2, 131.2, 136.3 (4 x ArCH), 140.3 (H_αC=CH_βC_q), 146.1 (H_αC=CH_β), 167.8 (C=O). The carbon atom (ArC_q-B) is not visible. ¹¹B-NMR

(dissolved in CDCl₃, 96 MHz) δ 31.5. HRMS (ESI⁺): For C₁₆H₂₂BO₄ [M + H]⁺ required 289.15448; found 289.16064. ATR-IR (ν , cm⁻¹) 3058 (w, ArC-H), 2980, 2945 (w, alkyl C-H), 1721 (s, C=O), 1635, 1593 (m, C=C), 1434 (m, C-B), 1345, 1323 (s, sp² B-O), 1143 (s, C-O), 772 (m, =C-H), 649 (s, C-H (ortho-disubstituted)).

(E)-Methyl 3-(3-(4,4,5,5-tetramethyl-1,3,2-dioxaborolan-2-yl)phenyl)acrylate *meta* 2

3-(4,4,5,5-Tetramethyl-1,3,2-dioxaborolan-2-yl)benzaldehyde ***meta* 1** (2.000 g, 8.618 mmol) was carefully added to

(methoxycarbonylmethylene)triphenylphosphorane (3.170 g, 9.479 mmol) stirring in a round bottom flask at r.t. The temperature was raised to 150°C and the powdery mixture liquefied and stirred as a pale yellow solution for 2.5 hours. The solution was allowed to cool down and turned into a tough pale yellow solid which was dissolved in DCM, transferred into a 500 mL round-bottom flask and evaporated in vacuo. TLC analysis (ethyl acetate/cyclohexane 1:4) revealed the presence of one product (R_f 0.70) and the byproduct triphenylphosphine oxide (R_f 0.10). Trituration with hexane and filtration allowed to remove a first crop of the byproduct triphenylphosphine oxide. The filtrate was left to stand overnight and a second crop of triphenylphosphine oxide crystallised. The hexane layer was decanted off and evaporated in vacuo to give a crystalline solid. Recrystallisation from petroleum ether 60/80 allowed to completely remove the triphenylphosphine oxide byproduct which crashed out. The product was obtained via evaporation of the filtrate fraction to give ***meta* 2** (2.210g, 89%) as a white crystalline solid. NMR analysis revealed a *E:Z* ratio across the double bond of 99:1. M.p. 108-112°C. ¹H-NMR (400MHz, CDCl₃) δ 1.36 (s, 12H, 4 x CH₃), 3.80 (s, 3H, OCH₃), 6.49 (d, 1H, ³J_{H α ,H β 16.0 Hz, H α -C=CH β), 7.39}

(t, 1H, 3J 7.6 Hz, ArH), 7.60 (d, 1H, 3J 7.6 Hz, ArH), 7.71 (d, 1H, $^3J_{H\beta, H\alpha}$ 16.0 Hz, $H\beta$ -C=CH α), 7.81 (d, 1H, 3J 7.6 Hz, ArH), 7.98 (s, 1H, C $_q$ ArCHC $_q$). ^{13}C -NMR (100MHz, CDCl $_3$) δ 25.0 (4 x CH $_3$), 51.8 (OCH $_3$), 84.2 (2 x C $_q$ -(CH $_3$) $_2$), 118.0 ($H\beta$ C=CH α), 128.4, 130.9 (2 x ArCH), 133.9 ($H\alpha$ C=CH β C $_q$), 136.7 (2 x ArCH), 145.0 ($H\alpha$ C=CH β), 167.6 (C=O). The carbon atom (ArC $_q$ -B) is not visible. ^{11}B -NMR (dissolved in CDCl $_3$, 96 MHz) δ 30.7. HRMS (ESI $^+$): For C $_{16}$ H $_{22}$ BO $_4$ [M + H] $^+$ required 289.15448; found 289.16057. ATR-IR (ν , cm $^{-1}$) 2975, 2928, 2855 (w, alkyl C-H), 1705 (s, C=O), 1635, 1600 (m, C=C), 1417 (m, C-B), 1354 (s, sp 2 B-O), 1140 (s, C-O), 995 (m, =C-H), 698 (s, C-H (meta-disubstituted)).

(E)-Methyl 3-(4-(4,4,5,5-tetramethyl-1,3,2-dioxaborolan-2-yl)phenyl)acrylate *para* 2

4-(4,4,5,5-Tetramethyl-1,3,2-dioxaborolan-2-yl)benzaldehyde ***para* 1** (884 mg, 3.809 mmol) was carefully added to

(methoxycarbonylmethylene)triphenylphosphorane (1.400 g, 4.189 mmol) stirring in a round bottom flask at r.t. The temperature was raised to 150°C and the powdery mixture liquefied and stirred as a pale yellow solution for 2.5 hours. The solution was allowed to cool down and turned into a tough pale yellow solid which was dissolved in acetone, transferred into a 500 mL round-bottom flask and evaporated in vacuo. TLC analysis (ethyl acetate/cyclohexane 1:4) revealed the presence of one product (R $_f$ 0.70) and the byproduct triphenylphosphine oxide (R $_f$ 0.10). Trituration with hexane (50 mL) and filtration allowed to remove a first crop of the byproduct triphenylphosphine oxide. The filtrate was evaporated in vacuo and the product (E)-methyl 3-(4-(4,4,5,5-tetramethyl-1,3,2-dioxaborolan-2-yl)phenyl)acrylate ***para* 2** was purified by flash column chromatography (ethyl acetate/cyclohexane 1:4) to give

1.000 g (91%) as a colourless crystalline solid. NMR analysis revealed a *E:Z* ratio across the double bond of 92:8. M.p. 86-93°C. ¹H-NMR (400MHz, CDCl₃) δ 1.35 (s, 12H, 4 x CH₃), 3.81 (s, 3H, OCH₃), 6.49 (d, 1H, ³J_{Hβ,Hα} 16.0 Hz, H_β-C=CH_α), 7.51 (d, 2H, ³J 8.0 Hz, 2 x ArHs), 7.69 (d, 1H, ³J_{Hα, Hβ} 16.0 Hz, H_α-C=CH_β), 7.82 (d, 2H, ³J 8.0 Hz, 2 x ArHs). ¹³C-NMR (100MHz, CDCl₃) δ 25.0 (4 x CH₃), 51.9 (OCH₃), 84.2 (2 x C_q-(CH₃)₂), 118.8 (H_βC=CH_α), 127.4 (2 x ArC_qCH), 134.6 (2 x ArC_qCH), 137.0 (C_q-CH=CH), 144.9 (H_αC=CH_β), 167.5 (C=O). The carbon atom (ArC_q-B) is not visible. ¹¹B-NMR (dissolved in CDCl₃, 96 MHz) δ 31.2. HRMS (ESI⁺): For C₁₆H₂₂BO₄ [M + H]⁺ required 289.15448; found 289.16075. ATR-IR (ν, cm⁻¹) 2979, 2944 (w, alkyl C-H), 1723 (s, C=O), 1639, 1608 (m, C=C), 1431 (m, C-B), 1358, 1312, 1088 (s, sp² B-O), 1141 (s, C-O), 1004 (m, =C-H), 826 (s, C-H (para-disubstituted)).

Conclusions

Three borylated derivatives of methyl cinnamate were produced via a green chemistry protocol with the best set of stereoisomeric ratios to date. They were fully characterized, including by X-ray crystallography, principally to study the behaviour of the boronate group. The drugs proved their glycosidase modulation capability to produce selective inhibition against a β-glucosidase and a β-galactosidase. Furthermore these compounds were screened against a panel of cancer cells and a normal cell line to ascertain their percent cell growth inhibition capabilities in view to their use as BNCT agents with the potential to fine-tune the timing of toxicity delivery.

Conflicts of interest

There are no conflicts to declare.

Acknowledgements

The B18 Project and, at the University of Newcastle, the Faculty of Science and the Priority Research Centre for Drug Development are gratefully acknowledged for research funding. Dr Robert Nash and Barbara Bartholomew at Phytoquest Ltd are gratefully acknowledged for running the assay against *N*-acetyl- β -D-glucosidase (bovine liver).

Supporting Information

X-Ray crystallography data and a table of synthetic strategies to cinnamates are available.

References

- (1) Byrne, P. A.; Gilheany, D. G. The Modern Interpretation of the Wittig Reaction Mechanism. *Chem. Soc. Rev.* **2013**, *42*, 6670-6696.
- (2) Bisceglia, J. A.; Orelli, L. R. Recent Progress in the Horner-Wadsworth-Emmons Reaction. *Curr. Org. Chem.* **2015**, *19*, 744-755.
- (3) Wadsworth, W. S. Synthetic Applications of Phosphoryl-Stabilized Anions. *Org. React.* **1977**, *25*, 73-253.
- (4) Jenkinson, S. F.; Thompson, A. L.; Simone, M. I. Methyl 2-(5,5-dimethyl-1,3,2-dioxaborinan-2-yl)-4-nitrobenzoate. *Acta Cryst.* **2012**, *E68*, o2429-o2430.
- (5) Pappin, B. B.; Levonis, S. M.; Healy, P. C.; Kiefel, M. J.; Simone, M. I.; Houston, T. A. Crystallization-induced Amide Bond Formation creates a Boron-centered Spirocyclic System. *Heterocyclic Commun.* **2017**, *23*, 167-169.
- (6) Simone, M. I.; Houston, T. A. A Brief Overview of Recent Advances in the Applications of Boronic Acids Relevant to Glycomics. *J. Glycomics & Lipidomics* **2014**, e124-e128
- (7) Perez, M. E.; Haramboure, M.; Mirande, L.; Romanelli, G. P.; Schneider, M. I.; Autino, J. C. Biological Activity of Three Alkyl Cinnamates on young Larvae of *Tuta absoluta*. *Commun. Agric. Appl. Biol. Sci.* **2013**, 299-303.
- (8) Zhu, J.; Majinika, M.; Tawata, S. Synthesis and Biological Activities of Pyranyl-substituted Cinnamates. *Biosci. Biotechnol. Biochem.* **2001**, *65*, 161-163.
- (9) Kong, J.-O.; Lee, S.-M.; Moon, Y.-S.; Lee, S.-G.; Ahn, Y.-J. Nematicidal activity of cassia and cinnamon oil compounds and related compounds toward *Bursaphelenchus xylophilus* (Nematoda: Parasitaphelenchidae). *J. Nematology* **2007**, *39*, 31-36.

- (10) Stefanović, O. D.; Radojević, I. D.; Čomić, L. R. Synthetic cinnamates as potential antimicrobial agents. *Hem. Ind.* **2015**, *69*, 37-42.
- (11) Tanachatchairatana, T.; Bremner, J. B.; Chokchaisiri, R.; Suksamrarn, A. Antimycobacterial activity of cinnamate-based esters of the triterpenes betulinic, oleanolic and ursolic acids. *Chem. Pharm. Bull.* **2008**, *56*, 194-198.
- (12) Guzman, J. D. Natural Cinnamic Acids, Synthetic Derivatives and Hybrids with Antimicrobial Activity. *Molecules* **2014**, *19*, 19292-19349.
- (13) Adisakwattana, S.; Sookkongwaree, K.; Roengsumran, S.; Petsom, A.; Ngamrojnavanich, N.; Chavasiri, W.; Deesamer, S.; Yibchok-Anun, S. Structure-activity relationships of trans-cinnamic acid derivatives on alpha-glucosidase inhibition. *Bioorg. Med. Chem. Lett.* **2004**, *14*, 2893-2896.
- (14) Prichard, K.; Campkin, D.; O'Brien, N.; Kato, A.; Fleet, G. W. J.; Simone, M. I. Biological activities of 3,4,5-trihydroxypiperidines and their N- and O-derivatives. *Chem. Biol. Drug Des.* **2018**, *92*, 1171-1197.
- (15) Simone, M. I.; Mares, L. J.; Eveleens, C. A.; McCluskey, A.; Pappin, B. B.; Kiefel, M. J.; Houston, T. A. Back to (non-)Basics: An Update on Neutral and Charge-Balanced Glycosidase Inhibitors. *Mini-Rev. Med. Chem.* **2018**, *18*, 812-827.
- (16) Balema, V. P.; Wiench, J. W.; Pruski, M.; Pecharsky, V. K. Mechanically Induced Solid-State Generation of Phosphorus Ylides and the Solvent-Free Wittig Reaction. *J. Am. Chem. Soc.* **2002**, *124*, 6244-6245.
- (17) Leung, S. H.; Angel, S. A. Solvent-Free Wittig Reaction: A Green Organic Chemistry Laboratory Experiment. *J. Chem. Educ.* **2004**, *81*, 1492-1493.
- (18) Shockravi, A.; Valizadeh, H.; Heravi, M. M. A One-pot Convenient Synthesis of Coumarins in Solventless Systems. *Phosphorus Sulfur Silicon Relat. Elem.* **2003**, *178*, 501-504.
- (19) Liu, W.-Y.; Xu, Q.-H.; Ma, Y.-X.; Liang, Y.-M.; Dong, N.-L.; Guan, D.-P. Solvent-free synthesis of ferrocenylethene derivatives. *J. Organomet. Chem.* **2001**, *625*, 128-131.
- (20) Hu, Z.-J.; Sun, P.-P.; Li, L.; Tian, Y.-P.; Yang, J.-X.; Wu, J.-Y.; Zhou, H.-P.; Tao, L.-M.; Wang, C.-K.; Li, M.; Cheng, G.-H.; Tang, H.-H.; Tao, X.-T.; Jiang, M.-H. Two novel π -conjugated carbazole derivatives with blue two-photon-excited fluorescence. *Chem. Phys.* **2009**, *355*, 91-98.
- (21) Nguyen, K. C.; Weizman, H. Greening Wittig Reactions: Solvent-Free Synthesis of Ethyl trans-Cinnamate and trans-3-(9-Anthryl)-2-Propenoic Acid Ethyl Ester. *J. Chem. Educ.* **2007**, *81*, 119-121.
- (22) Texier-Boullet, F.; Villemin, D.; Ricard, M.; Moison, H.; Foucaud, A. Reactions de Wittig, Wittig-horner et Knoevenagel par Activation Anionique avec l'Alumine ou le Fluorure de Potassium depose sur l'Alumine, sans Solvant. *Tetrahedron* **1985**, *41*, 1259-1266.
- (23) Thiemann, T.; Watanabe, M.; Tanaka, Y.; Mataka, S. Solvent-Free Wittig Olefination with Stabilized Phosphoranes—Scope and Limitations. *New J. Chem.* **2004**, *28*, 578-584.
- (24) Watanabe, M.; Morais, G. R.; Mataka, S.; Ideta, K.; Thiemann, T. Two Variations of Solvent-Reduced Wittig Olefination Reactions – Comparison of Solventless Wittig Reactions to Wittig Reactions under Ultrasonication with Minimal Work-up. *Z. Naturforschung* **2005**, *60b*, 909-915.
- (25) Sadeq, H.; Thiemann, T.; Graham, J. P.; Jasem, Y.; Bugenhagen, B.; Al-Rawashdeh, N.; Sulaidi, M. Preparation of 3-(9-Anthryl) acrylates and 9-Aroylethenylantracenes as π -Extended Anthracenes and Their Diels–Alder Type Adducts with Electron-Poor Dienophiles. *Polycyclic Arom. Comp.* **2016**, *37*, 148-160.

- (26) Shanmugavelan, P.; Sathishkumar, M.; Nagarajan, S.; Ranganathan, R.; Ponnuswamy, A. The First Solvent- Free, Microwave- Accelerated, Three- Component Synthesis of Thiazolidin- 4- ones via One- Pot Tandem Staudinger/aza- Wittig Reaction. *J. Heterocyclic Chem.* **2014**, *51*, 1004-1011.
- (27) Ponnuswamy, A.; Shanmugavelan, P.; Nagarajan, S.; Sathishkumar, M. The First One- Pot, Solvent- Free, Microwave- Accelerated, Three- Component Synthesis of Spirothiazolidin- 4- ones via *Staudinger/Aza- Wittig* Coupling/Cyclization. *Helv. Chi. Acta* **2012**, *95*, 922-928.
- (28) Pappin, B. B.; Garget, T. A.; Healy, P. C.; Simone, M. I.; Kiefel, M. J.; Houston, T. A. Facile Amidinations of 2-Aminophenylboronic Acid promoted by Boronate Ester Formation. *Org. Biomol. Chem.* **2019**, *17*, 803-806.
- (29) Hitosugi, S.; Tanimoto, D.; Nakanishi, W.; Isobe, H. A facile chromatographic method for purification of pinacol boronic esters. *Chem. Lett.* **2012**, *41*, 972-973.
- (30) Lautens, M.; Mancuso, J. Addition of Bifunctional Organoboron Reagents to Strained Alkenes. Carbon–Carbon Bond Formation with Rh(I) Catalysis in Aqueous Media. *J. Org. Chem.* **2004**, *69*, 3478-3487.
- (31) Rasina, D.; Otkovs, M.; Leitans, J.; Recacha, R.; Borysov, O. V.; Kanepe-Lapsa, I.; Domraceva, I.; Pantelejevs, D.; Tars, K.; Blackman, M. J.; Jaudzems, K.; Jirgensons, A. Fragment-based Discovery of 2-Aminoquinazolin-4(3h)-ones as Novel Class Nonpeptidomimetic Inhibitors of the Plasmepsins I, II, and IV. *J. Med. Chem.* **2016**, *59*, 374-387.
- (32) Molander, G. A.; Oliveira, R. A. Wittig Reaction of Formyl-substituted Organotrifluoroborates and Stabilized Phosphonium Ylides in an Aqueous Medium. *Tetrahedron Lett.* **2008**, *49*, 1266-1268.
- (33) Campo, V. L.; Aragão- Leoneti, V.; Carvalho, I. *Carbohydrate Chemistry: Volume 39. Glycosidases and diabetes: metabolic changes, mode of action and therapeutic perspectives*; Royal Society of Chemistry, 2013.
- (34) Qu, X.; Pan, X.; Weidner, J.; Yu, W.; Alonzi, D.; Xu, X.; Butters, T.; Block, T.; Guo, J.-T.; Chang, J. Inhibitors of Endoplasmic Reticulum alpha-Glucosidases Potently Suppress Hepatitis C Virus Virion Assembly and Release. *Antimicrob. Agents Chemother.* **2011**, *55*, 1036-1044.
- (35) Greiner-Tollersrud, O. K.; Berg, T. *Lysosomal Storage Disorders*; Landes Bioscience: Austin (Texas), 2013.
- (36) Johnson, L. L.; Houston, T. A. A Drug targeting Motif for Glycosidase Inhibitors: an Iminosugar–boronate shows unexpectedly selective β -Galactosidase Inhibition. *Tetrahedron Lett.* **2002**, *43*, 8905-8908.
- (37) Windsor, I. W.; Palte, M. J.; III, J. C. L.; Gold, B.; Forest, K. T.; Raines, R. T. Sub-Picomolar Inhibition of HIV-1 Protease with a Boronic Acid. *J. Am. Chem. Soc.* **2018**, *140*, 14015-14018.
- (38) Lovering, F.; Bikker, J.; Humblet, C. Escape from Flatland: Increasing Saturation as an Approach to Improving Clinical Success. *J. Med. Chem.* **2009**, *52*, 6752-6756.
- (39) Yang, F.; Zhu, M.; Zhang, J.; Zhou, H. Synthesis of Biologically Active Boron-containing Compounds. *Med. Chem. Commun.* **2018**, *9*, 201-211.
- (40) Baker, S. J.; Ding, C. Z.; Akama, T.; Zhang, Y. K.; Hernandez, V.; Xia, Y. Therapeutic Potential of Boron-containing Compounds. *Future Med. Chem.* **2009**, *1*, 1275-1288.
- (41) Glenister, A.; Simone, M. I.; Hambley, T. W. A Warburg Effect targeting Vector designed to increase the Uptake of Compounds by Cancer Cells demonstrates Glucose and Hypoxia dependent Uptake. *PlosOne* **2019**, e0217712.

- (42) Yamamoto, T.; Nakai, K.; Matsumura, A. Boron Neutron Capture Therapy for Glioblastoma. *Cancer Lett.* **2008**, 262, 143-152.
- (43) Zavjalov, E.; Zaboronok, A.; Kanygin, V.; Kasatova, A.; Kichigin, A.; Mukhamadiyarov, R.; Razumov, I.; Sycheva, T.; Mathis, B. J.; Maezono, S. E. B.; Matsumura, A.; Taskaev, S. Accelerator-based Boron Neutron Capture Therapy for Malignant Glioma: a Pilot Neutron Irradiation Study using Boron Phenylalanine, Sodium Borocaptate and Liposomal Borocaptate with a Heterotopic U87 Glioblastoma Model in SCID Mice. *Internat. J. Radiation Biol.* **2020**, 868-878.
- (44) Nakagawa, Y.; Pooh, K.; Kobayashi, T.; Kageji, T.; Uyama, S.; Matsumura, A.; Kumada, H. Clinical Review of the Japanese Experience with Boron Neutron Capture Therapy and a Proposed Strategy using Epithermal Neutron Beams. *J. Neuro-Oncol.* **2003**, 62, 87-99.
- (45) "INEL BNCT Research Program Annual Report," INEL Lockheed Idaho Technologies Company, **1995**.
- (46) Koo, M.-S.; Ozawa, T.; Santos, R. A.; Lamborn, K. R.; Bollen, A. W.; Deen, D. F.; Kahl, S. B. Synthesis and Comparative Toxicology of a Series of Polyhedral Borane Anion-Substituted Tetraphenyl Porphyrins. *J. Med. Chem.* **2007**, 50, 820-827.
- (47) Cano, W. G.; Solares, G. R.; Dipetrillo, T. A.; Meylaerts, S. A. G.; Lin, S. C.; Zamenhof, R. G.; Saris, S. C.; Duker, J. S.; Goad, E.; Madoc- Jones, H.; Wazer, D. E. Toxicity Associated with Boronophenylalanine and Cranial Neutron Irradiation. *Radiation Oncology Investigations* **1995**, 3, 108-118.
- (48) Uluisika, I.; Karakaya, H. C.; Koc, A. The Importance of Boron in Biological Systems. *J. Trace Elem. Med. Biol.* **2018**, 45, 156-162.
- (49) U.S. Department of Health and Human Services, Public Health Service Agency for Toxic Substances and Disease Registry. "Toxicological profile for benzene," August **2007**.
- (50) <https://www.cdc.gov/niosh/idlh/71432.html>. Accessed in November 2020.
- (51) https://m.chemicalbook.com/ChemicalProductProperty_EN_CB5323625.htm. Accessed July 2020.
- (52) Gottlieb, H. E.; Kotlyar, V.; Nudelman, A. NMR Chemical Shifts of Common Laboratory Solvents as Trace Impurities. *J. Org. Chem.* **1997**, 62, 7512-7515.
- (53) Sheldrick, G. M. A short history of SHELX. *Acta Cryst.* **2008**, A64, 112-122.
- (54) Macrae, C. F.; Edgington, P. R.; McCabe, P.; Pidcock, E.; Shields, G. P.; Taylor, R.; Towler, M.; van der Streek, J. Mercury Visualization and Analysis of Crystal Structures. *J. Appl. Crystallogr.* **2006**, 39, 453-457.
- (55) Spek, A. L. Single-crystal structure validation with the program PLATON. *J. Appl. Crystallogr.* **2003**, 36, 7-13.